High-Temperature Measurements of the Reactions of OH with Toluene and Acetone

Venkatesh Vasudevan,* David F. Davidson, and Ronald K. Hanson

High Temperature Gasdynamics Laboratory, Mechanical Engineering Department, Stanford University, Stanford, California 94305

Received: January 7, 2005; In Final Form: February 24, 2005

The reaction of hydroxyl [OH] radicals with toluene [$C_6H_5CH_3$] was studied at temperatures between 911 and 1389 K behind reflected shock waves at pressures of ~2.25 atm. OH radicals were generated by rapid thermal decomposition of shock-heated *tert*-butyl hydroperoxide [$(CH_3)_3-CO-OH$], and monitored by narrow-line width ring dye laser absorption of the well-characterized $R_1(5)$ line of the OH A−X (0,0) band near 306.7 nm. OH time histories were modeled by using a comprehensive toluene oxidation mechanism. Rate constants for the reaction of $C_6H_5CH_3$ with OH were extracted by matching modeled and measured OH concentration time histories in the reflected shock region. Detailed error analyses yielded an uncertainty estimate of ±30% at 1115 K for the rate coefficient of this reaction. The current high-temperature data were fit with the lower temperature measurements of Tully et al. [*J. Phys. Chem.* **1981**, *85*, 2262−2269] to the following two-parameter form, applicable over 570−1389 K: $k_3 = (1.62 \times 10^{13}) \exp(-1394/T\ [\mathrm{K}])$ [$\mathrm{cm^3\ mol^{-1}\ s^{-1}}$]. The reaction between OH radicals and acetone [CH_3COCH_3] was one of the secondary reactions encountered in the toluene + OH experiments. Direct high-temperature measurements of this reaction were carried out at temperatures ranging from 982 to 1300 K in reflected shock wave experiments at an average total pressure of 1.65 atm. Uncertainty limits were estimated to be ±25% at 1159 K. A two-parameter fit of the current data yields the following rate expression: $k_6 = (2.95 \times 10^{13}) \exp(-2297/T\ [\mathrm{K}])$ [$\mathrm{cm^3\ mol^{-1}\ s^{-1}}$].

Introduction

Aromatics are a major constituent of commercial gasoline and aviation fuels. The addition of aromatics to gasoline reduces the propensity to knocking and increases the fuel octane number.[1] Also, fuel components such as toluene and xylene have the desirable properties of high energy rating and high knock rating.[2,3]

A limited number of kinetic studies of toluene oxidation[4−9] have been reported in the literature. Despite toluene's importance as a key fuel component, the high-temperature combustion of this aromatic is not very well understood, and there is much uncertainty associated with rate coefficients of several of the key reactions that are rate-controlling in the oxidation of toluene at elevated temperatures. Accurate, detailed kinetic models are essential for the prediction of global phenomena of interest such as autoignition, and premixed and nonpremixed burning of toluene and gasoline in internal combustion engines.[7]

In recent work,[10] we studied toluene chemistry by carrying out detailed measurements of OH radical time histories during toluene oxidation, with the objective of providing unique kinetic targets for chemical model development and validation. The performance of three currently available toluene oxidation mechanisms[6−8] was analyzed by comparing the measured ignition time and OH time history data to model predictions. Figure 1a presents a typical OH concentration time history measurement, along with detailed model calculations using the Pitz et al. toluene oxidation mechanism,[7] for a stoichiometric 1000 ppm toluene−oxygen mixture dilute in argon. An OH radical sensitivity analysis, for the conditions of this experiment, 1586 K and 1.9 atm, is shown in Figure 1b. As is evident, the reactions with the greatest sensitivity at early times are:

$$H + O_2 \rightarrow O + OH \quad (1)$$

$$C_6H_5CH_3 + H \rightarrow C_6H_5CH_2 + H_2 \quad (2)$$

$$C_6H_5CH_3 + OH \rightarrow \text{products} \quad (3)$$

$$C_6H_5CH_3 \rightarrow C_6H_5CH_2 + H \quad (4)$$

$$C_6H_5CH_3 \rightarrow C_6H_5 + CH_3 \quad (5)$$

The differences between simulation and experiment, with regard to OH plateau levels, ignition delay, and early-time behavior, may be attributed, in part, to discrepancies in the rate coefficients of the above reactions.[10]

Reaction 1 is by far the most sensitive reaction over the entire time frame of the experiment shown in Figure 1. There have been several studies of reaction 1 reported over the years, and recent publications[12] estimate an uncertainty of just 9% for this rate coefficient over the 1336−3370 K temperature range.

Reaction 2, the abstraction of an H atom from the methyl group in toluene by H, is known[13] to within a factor of 2. The current estimate on the uncertainty of reaction 3 is relatively large,[13] a factor of 3.16. While the reaction of OH radicals with toluene has been studied at low temperatures[14−17] because of its importance in tropospheric pollution, extensive kinetic measurements of this reaction have not been made at elevated temperatures. To our knowledge, there has been only one direct kinetic investigation of this reaction at temperatures greater than 500 K,[15] and none at temperatures greater than 1050 K. Investigations at higher temperatures appear to be warranted. There have been numerous measurements of reactions 4 and 5 [see, for example, refs 18 and 19 and references therein], and rate coefficients for these reactions are reasonably well established at their high-pressure limits; but, there has been only one

* Corresponding author. Phone: 650-725-2042. Fax: 650-723-1748. E-mail: venkv@stanford.edu.

10.1021/jp0501143 CCC: $30.25
Published on Web 03/30/2005

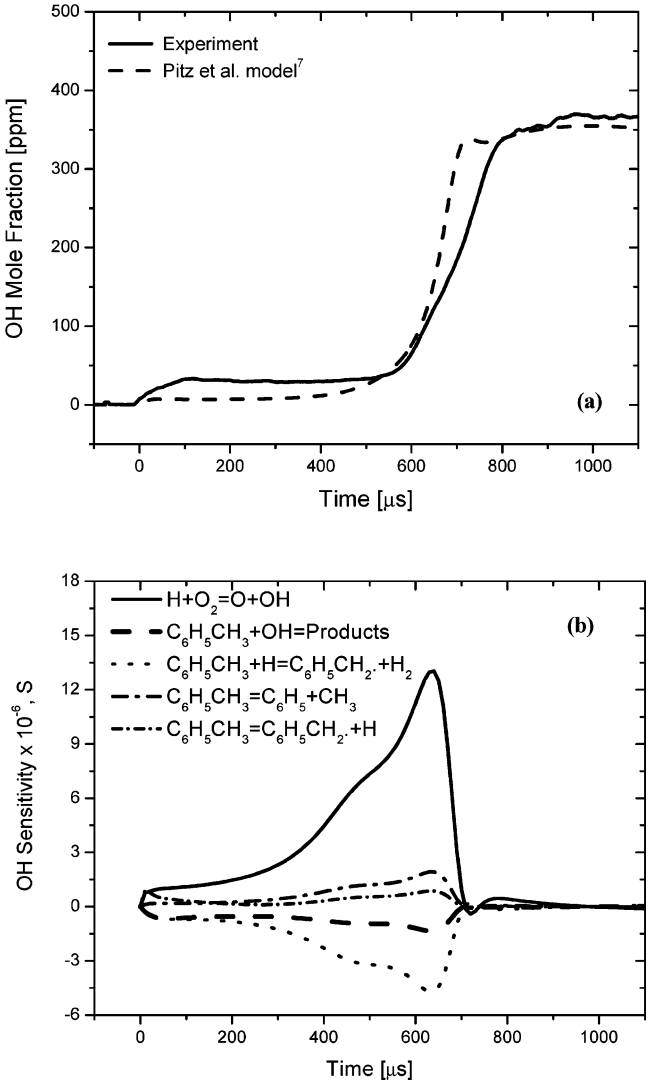

Figure 1. Initial reflected shock conditions: 1586 K, 1.9 atm; 0.1% $C_6H_5CH_3$, 0.9% O_2, $\varphi = 1$: (a) typical OH concentration time history during toluene oxidation and (b) OH radical sensitivity analysis, $S = (dX_{OH}/dk_i)(k_i)$.

shock tube study of this reaction system at low pressures.[18] While measurements of toluene decomposition in the "falloff" regime are currently planned, in this paper we describe direct, high-temperature measurements of the reaction between toluene and OH radicals.

OH radicals were generated by shock heating *tert*-butyl hydroperoxide [$(CH_3)_3$-CO-OH], and monitored by narrow-line width ring dye laser absorption at 306.7 nm. A comprehensive toluene oxidation mechanism[7] was used to model the OH time histories. The mechanism was assembled by adding to the C1−C4 mechanism of Curran et al.[24] the toluene and benzene reaction mechanism of Zhong et al.[25−27] Further details on the mechanism are available elsewhere.[7] Rate constants for the reaction between $C_6H_5CH_3$ and OH were extracted by varying this rate to achieve a match between modeled and measured OH concentration time histories behind reflected shocks, over the 911−1389 K temperature range.

The reaction between OH radicals and acetone [CH_3COCH_3], reaction 6, was one of the secondary reactions encountered in the toluene + OH experiments.

$$CH_3COCH_3 + OH \rightarrow CH_3COCH_2 + H_2O \qquad (6)$$

Even though the kinetics of OH radical attack on acetone is of importance in combustion systems, there is scarcity of high-temperature data on reaction 6. There has been only a single, direct high-temperature measurement of this reaction rate coefficient, made at 1200 K, in a shock tube;[20] data at elevated temperatures are clearly needed. Here, we report rate coefficient data for this reaction at temperatures ranging from 982 to 1300 K.

TABLE 1: $C_6H_5CH_3$ + OH → Products: Rate Coefficient Data

T_5 [K]	P_5 [atm]	k_3 [cm^3 mol^{-1} s^{-1}]
100 ppm TBHP (and water), 120 ppm $C_6H_5CH_3$, Ar		
911	2.82	3.14×10^{12}
972	2.74	3.35×10^{12}
1069	2.49	4.29×10^{12}
1115	2.44	4.54×10^{12}
1174	2.39	4.86×10^{12}
1277	2.22	5.23×10^{12}
1344	2.15	6.19×10^{12}
1389	2.07	7.10×10^{12}
100 ppm TBHP (and water), 240 ppm $C_6H_5CH_3$, Ar		
1093	2.48	4.42×10^{12}
1281	2.18	5.84×10^{12}

TABLE 2: CH_3COCH_3 + OH → CH_3COCH_2 + H_2O: Rate Coefficient Data

T_5 [K]	P_5 [atm]	k_6 [cm^3 mol^{-1} s^{-1}]
200 ppm TBHP (and water), 504 ppm CH_3COCH_3, Ar		
1093	1.57	3.46×10^{12}
1159	1.61	4.14×10^{12}
1188	1.58	4.31×10^{12}
1201	1.52	4.05×10^{12}
1297	1.80	5.42×10^{12}
1300	1.54	4.98×10^{12}
200 ppm TBHP (and water), 486 ppm CH_3COCH_3, Ar		
982	1.85	2.87×10^{12}
1048	1.77	3.35×10^{12}
1260	1.57	4.55×10^{12}

A total of 19 kinetic measurements (see Tables 1 and 2) were carried out to ascertain rate coefficients for the reactions of OH with $C_6H_5CH_3$ and CH_3COCH_3. Modeled OH traces were fit to the measurements over a time window of ∼75 μs. In this time frame the OH profiles show maximum sensitivity to reactions 3 and 6, and hence yield rate data under conditions where the reactions of interest are almost completely isolated chemically. In all the modeling carried out in this work, the recently revised value for the standard heat of formation of OH was used.[11]

Experimental Setup

Experiments were carried out in the reflected shock region of a high-purity, stainless steel, helium-driven shock tube with inner diameter of 15.24 cm and length 10.5 m. Research grade argon (99.999%) was supplied by Praxair Inc. A commercially available solution of 70% *tert*-butyl hydroperoxide (TBHP) in water from Sigma Aldrich was used in the experiments conducted. Research grade toluene (>99.5%) and acetone (>99.5%) were supplied by Aldrich Chemical Co., Inc. and purified before use by a freeze−thaw procedure. Mixtures were prepared manometrically in a 14 L stainless steel mixing chamber equipped with a magnetic stirrer assembly and mixed for about 2 h to ensure homogeneity and consistency. Before shock heating, mixture samples were analyzed in a gas chromatograph (SRI GC 8160-C), providing a check on possible decomposition of TBHP in the gas phase in the mixing chamber. It was found that less than 0.30 ppm of TBHP decomposes in the mixing tank to form acetone.[21] Modeling the reaction system with the decomposition taken into account showed that this has no discernible effect on our rate measurements.

The shock tube test section was evacuated before each run with a turbo-molecular pump (Varian V1000) to pressures on the order of 10^{-7} Torr. Incident shock velocity measurements were made by using five PZT pressure transducers (PCB) and four programmable timer counters (Fluke PM6666) and linearly extrapolated to the endwall. Average attenuation rates were between 0.6% and 1.1% per meter. Ideal shock relations and thermodynamics data from the Sandia database[22] were used to calculate reflected shock temperature and pressure. The thermodynamic database was updated with properties for toluene, acetone, and TBHP.[7] Further details of the shock tube setup can be found elsewhere.[10,11,21]

OH radicals were monitored using a narrow-line width ring dye laser tuned to the center of the $R_1(5)$ absorption line in the OH A−X (0,0) band near 306.7 nm. Twenty five to thirty milliwatts of visible light at 613.4 nm was generated in a Spectra-Physics 380 ring dye laser cavity by pumping Rhodamine 6G dye with a 5 W, 532 nm, cw beam produced by a Coherent (Verdi) laser. The visible light beam was then intracavity frequency-doubled in a temperature-tuned AD*A crystal to generate 1−2 mW of UV light at 306.7 nm. The wavelength of the visible light beam was monitored with a Burleigh WA-1000 wavemeter. Uncertainty in the wavemeter reading is estimated to be 0.01 cm^{-1} in the UV, and this was taken into account when fitting uncertainty estimates on our rate measurements. A part of the UV beam was split off upstream of the diagnostic section of the shock tube and common mode rejection of laser intensity fluctuations was performed by balancing the two beams (transmitted and reference) with a neutral density filter. The minimum absorption detection limit was less than 0.1%, leading to ppm-level detectivities for OH at microsecond time scales. OH was monitored 2 cm from the end wall of the shock tube with UV grade CaF_2 windows. Well-known absorption coefficients for OH were used in Beer's law to generate quantitative OH concentration profiles from the raw traces of fractional transmission. Off-line measurements did not reveal any interference (background) absorption.

In situ toluene concentration measurements, carried out with a 3.39 μm He−Ne diagnostic,[23] indicate that less than 10% of the initial toluene test gas is lost due to adsorption and condensation on the walls of the mixing assembly, manifold, and shock tube; this uncertainty in the initial toluene concentration was accounted for when determining error limits for our rate measurements. Evidence was also found for significant loss of TBHP in the mixing assembly and shock tube—these observations are described in the next section.

Kinetic Measurements

The reaction of toluene with hydroxyl radicals was studied at temperatures ranging from 911 to 1389 K, and at total pressures between 2.07 and 2.82 atm. Nominal mixtures with 100 ppm TBHP (and water) and 120−240 ppm toluene dilute in argon were prepared.

OH Precursor Kinetics. TBHP, the OH precursor used in this study, decomposes almost instantaneously upon shock heating above ~1000 K to form an OH radical and a *tert*-butoxy radical [$(CH_3)_3CO$]. The *tert*-butoxy radical subsequently falls apart rapidly to form acetone and a methyl radical. The decomposition pathways are:

$$(CH_3)_3\text{-}CO\text{-}OH \rightarrow (CH_3)_3CO + OH \quad (7)$$

$$(CH_3)_3CO \rightarrow CH_3COCH_3 + CH_3 \quad (8)$$

Reactions 7 and 8 were added to the Pitz et al. mechanism; rate coefficients suggested by Vasudevan et al.[21] and Benson [28,29] were used for these reactions. TBHP, unlike other OH precursors such as H_2O_2, HNO_3, and HNO_2, is relatively easy to handle, and rapidly dissociates at low temperatures of ~1000 K.[21,28] It is also quite stable on metal surfaces, evident from the results of the GC analyses that were described earlier in the paper.

Toluene + OH Kinetics. A sample OH concentration time history recorded on shock heating a mixture of 100 ppm TBHP (and water) and 120 ppm toluene in argon is shown in Figure 2a. Numerical simulations of the reaction system reveal that water in the initial mixture has no discernible effect on the measured OH profiles in our experimental range. For the conditions of the experiment shown, 1115 K and 2.44 atm, the measured peak OH yield is ~12 ppm (see Figure 2a), substantially lower than the potential maximum of ~30 ppm[21] estimated by using Raoult's law applied to the TBHP−water mixture. The lower than expected OH yield is attributed to condensation and adsorption of TBHP onto the walls of the mixing tank and shock tube. The measurement of OH provides a check on the actual concentration of TBHP in the shock tube. The assumption that condensation and adsorption reduce the mole fraction of TBHP from its nominal value is reasonable, especially because GC analyses indicate that there is little or no decomposition of TBHP in the gas phase in the mixing chamber. In model simulations, an initial TBHP mole fraction that resulted in the measured peak OH yield was used. For example, for the experiment presented in Figure 2a, an initial TBHP mole fraction of 12 ppm in the model leads to good agreement between the measured and modeled OH peaks.

An OH radical sensitivity analysis, presented in Figure 2b, clearly shows that the reactions between toluene and OH are the most sensitive over the entire time frame of the experiment. The chemistry is almost first order, with only slight interference from the following reactions:

$$CH_3COCH_3 + OH \rightarrow CH_3COCH_2 + H_2O \quad (6)$$

$$CH_3 + OH \rightarrow CH_2(S) + H_2O \quad (9)$$

$$CH_3OH\ (+M) \rightarrow CH_3 + OH\ (+M) \quad (10)$$

Measured and modeled OH time histories for one of our higher temperature experiments at 1344 K and 2.15 atm are presented in Figure 2c, while Figure 2d presents an OH sensitivity analysis for this experiment. It is evident that secondary chemistry is minimal—as with the lower temperature experiment presented above, interference is primarily due to reactions 6, 9, and 10, with slight, additional interference from reaction 11:

$$C_6H_5CH_2 + OH \rightarrow C_6H_5CH_2OH \quad (11)$$

A short discussion on the product pathways possible for the reaction between toluene and OH is pertinent here. In this study, three product channels were considered:

$$C_6H_5CH_3 + OH \rightarrow C_6H_5CH_2 + H_2O \quad (3a)$$

$$C_6H_5CH_3 + OH \rightarrow C_6H_4\,CH_3 + H_2O \quad (3b)$$

$$C_6H_5CH_3 + OH \rightarrow C_6H_5OH + CH_3 \quad (3c)$$

Tully et al.[15] assessed the relative importance of reactions 3a and 3b by assuming a ring-H abstraction rate coefficient, k_{3b}, that is five-sixths of the corresponding best-fit hydrogen

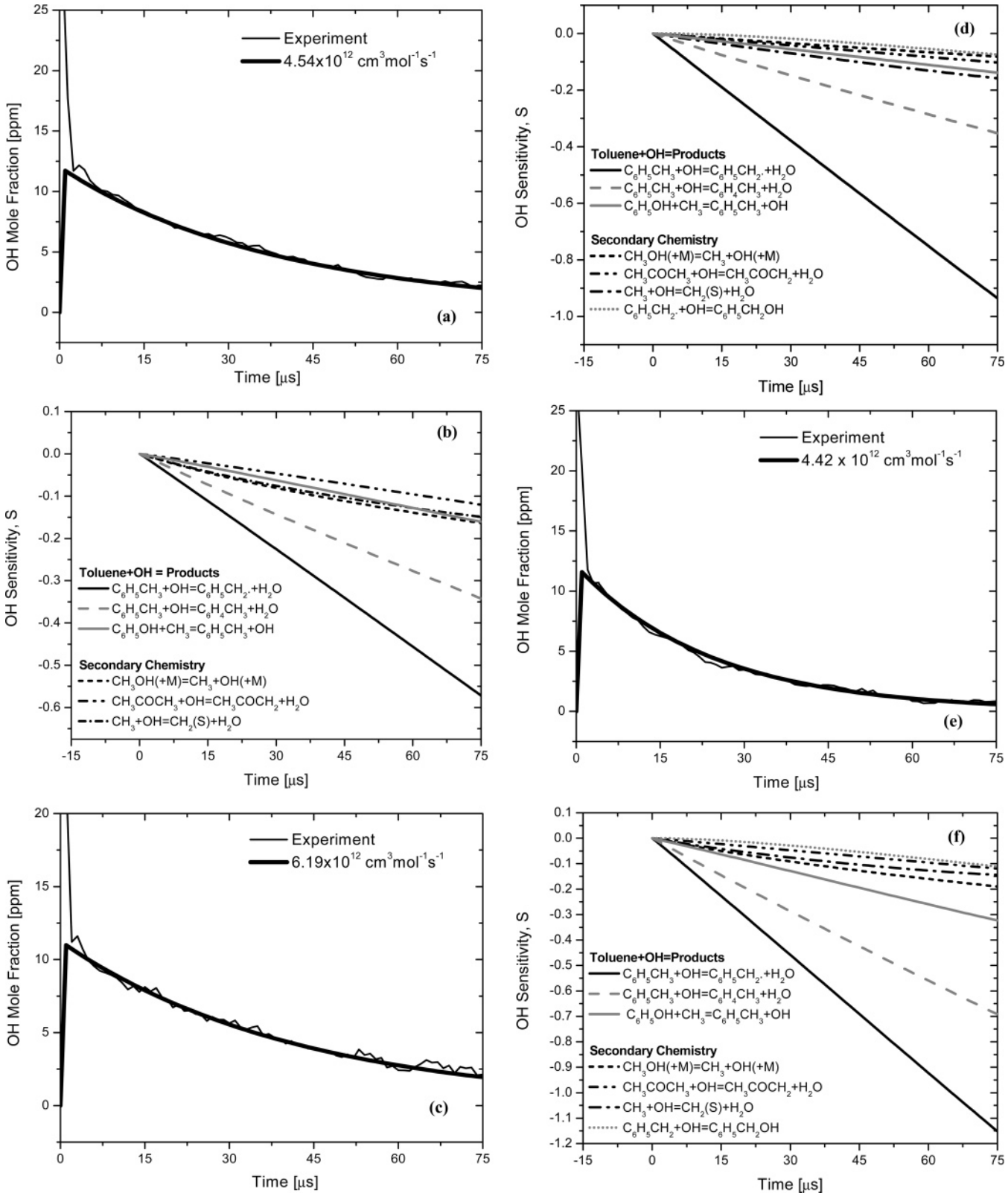

Figure 2. (a, b) Initial reflected shock conditions: 1115 K, 2.44 atm; 12 ppm TBHP, 120 ppm $C_6H_5CH_3$, Ar: (a) OH concentration time history and (b) OH radical sensitivity analysis, $S = (dX_{OH}/dk_i)(k_i/X_{OH})$. (c, d) Initial reflected shock conditions: 1344 K, 2.15 atm; 11.25 ppm TBHP, 120 ppm $C_6H_5CH_3$, Ar: (c) OH concentration time history and (d) OH radical sensitivity analysis, $S = (dX_{OH}/dk_i)(k_i/X_{OH})$. (e, f) Initial reflected shock conditions: 1093 K, 2.48 atm; 12 ppm TBHP, 240 ppm $C_6H_5CH_3$, Ar: (e) OH concentration time history and (f) OH radical sensitivity analysis, $S = (dX_{OH}/dk_i)(k_i/X_{OH})$.

abstraction rate constant for benzene. A point-by-point subtraction of k_{3b} from experimental measurements of the overall rate, k_3, was carried out. This yielded data on k_{3a}, the rate coefficient for side-chain hydrogen abstraction. Tully et al. found that $k_{3b}/k_{3a} \leq 0.5$ for all $T < 1500$ K, and this is consistent with what we would expect considering the relatively high bond energy for C−H in the aromatic ring. Investigations of the reactions of OH with four isotopically substituted toluenes also suggested that side-chain H abstraction, reaction 3a, is the dominant pathway for the reaction between OH and toluene at elevated

TABLE 3: Reactions Describing $C_6H_5CH_3$ + OH Experiments

reaction	rate coeff [cm^3 mol^{-1} s^1] A	n	E, cal/mol	ref
$(CH_3)_3$-CO-OH → $(CH_3)_3CO$ + OH	2.50×10^{15}	0.0	42 998	21
$(CH_3)_3CO$ → $CH_3COCH_3 + CH_3$	1.30×10^{14}	0.0	15 300	28, 29
$C_6H_5CH_3 + OH \rightarrow C_6H_5CH_2 + H_2O$		see text		this work
$C_6H_5CH_3 + OH \rightarrow C_6H_4CH_3 + H_2O$	1.20×10^{13}	0.0	4 491	15
$C_6H_5OH + CH_3 \rightarrow C_6H_5CH_3 + OH$	5.42×10^{14}	−0.83	12 100	7
$CH_3 + OH \rightarrow CH_2$ (S) + H_2O	2.65×10^{13}	0.0	2 186	7
$CH_3 + OH \rightarrow CH_2O + H_2$	2.25×10^{13}	0.0	4 300	7
$CH_3COCH_3 + OH \rightarrow CH_3COCH_2 + H_2O$		see text		this work
$CH_3COCH_3 \rightarrow CH_3CO + CH_3$	1.22×10^{23}	−1.99	83 950	7
$C_6H_5CH_2 + OH \rightarrow C_6H_5CH_2OH$	2.00×10^{13}	0.0	0	7
$O + H_2O \rightarrow OH + OH$	2.96×10^{6}	2.02	13 400	7
$2CH_3$ (+M) → C_2H_6 (+M)	9.21×10^{16}	−1.17	635.8	7
low-pressure limit: 0.113×10^{37}	−5.24	0.170×10^{4}		
Troe centering: 0.405	0.112×10^{4}	0.696×10^{2}	0.1×10^{16}	
CH_3OH (+M) → $CH_3 + OH$ (+M)	1.90×10^{16}	0.0	91 730	7
low-pressure limit: 0.295×10^{45}	−7.35	0.954×10^{5}		
Troe centering: 0.414	0.279×10^{3}	0.546×10^{4}	0.1×10^{101}	

temperatures.[15] In the present work, no attempt was made to determine quantitative rate expressions for these individual product channels. When fitting modeled traces to experiment, the dominant reaction pathway, assumed to be reaction 3a, was iteratively adjusted to yield a best fit, while the rate coefficients recommended by Tully et al.[15] and Pitz et al.[7] were used for the minor channels yielding phenylmethyl (reaction 3b) and phenol (reaction 3c). Reactions that are essential for the description of the toluene + OH experiments are summarized in Table 3 along with their rate parameters.

For the experiments shown in panels a and c of Figure 2, overall rate constants ($k_{3a} + k_{3b} + k_{3c}$) of 4.54×10^{12} and 6.19×10^{12} cm^3 mol^{-1} s^{-1}, respectively, for reaction 3 lead to excellent agreement between modeled and measured OH time histories. To confirm that our modeling is consistent, experiments were conducted with a higher toluene concentration in the initial mixture. An OH concentration profile obtained on shock heating a nominal mixture of 100 ppm of TBHP and 240 ppm of toluene dilute in argon is presented in Figure 2e, while Figure 2f shows an OH radical sensitivity analysis for the conditions of this experiment (1093 K and 2.48 atm). We note, from Figure 2f, that even with the higher fuel concentration mixture, interference from secondary reactions is minimal. Furthermore, the k_3 that leads to a best fit between the simulated and measured OH traces, 4.42×10^{12} cm^3 mol^{-1} s^{-1}, is entirely consistent with measurements made at comparable temperatures of 1069 and 1115 K. Table 1 summarizes the current measurements of the rate coefficient of $C_6H_5CH_3$ + OH → products.

A detailed error analysis was carried out to set uncertainty limits on the measured rate coefficients. The following uncertainty categories were considered: uncertainty in [a] wavemeter reading in the UV (0.01 cm^{-1}); [b] absorption coefficient of OH (± 3%); [c] mixture concentrations (±10%); [d] reflected shock temperature (±1%), primarily due to uncertainty in the shock velocity determination; [e] rate coefficients of secondary reactions [reactions 6, 9, and 10]; and, [f] fitting the modeled trace to the experimental profile. The major uncertainty categories and their effect on the target reaction rate, for the experiment at 1115 K and 2.44 atm, are shown in Figure 3. The effect of each of the above uncertainty categories on the rate coefficient of $C_6H_5CH_3$ + OH is ascertained and combined to yield an overall uncertainty estimate of ±30% at 1115 K and 2.44 atm. A slightly higher uncertainty of ±35% is estimated for our highest temperature measurements; this increase in the uncertainty comes about mainly due to interference from the reaction between benzyl and OH at elevated temperatures (see Figure 2d).

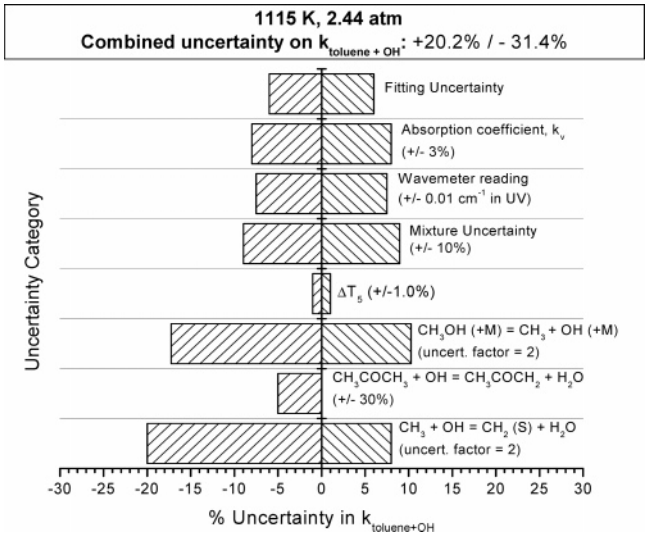

Figure 3. Uncertainty analysis for rate coefficient of $C_6H_5CH_3$ + OH → products; initial reflected shock conditions: 1115 K, 2.44 atm; individual error sources were applied separately and their effect on $k_{toluene+OH}$ was determined.

We note that ensuing secondary chemistry of the products formed via reactions 3a−3c could potentially interfere with an overall rate measurement for reaction 3. The Pitz et al. model already includes benzyl [$C_6H_5CH_2$] and phenol [C_6H_5OH] chemistry—secondary reactions due to these species are insignificant in our experimental regime (this is evident from Figure 2b), except for our highest temperature measurements where, as pointed out earlier, the reaction between benzyl and OH is slightly interfering (Figure 2d). Phenylmethyl [$C_6H_4CH_3$] yields are expected to be small in our experimental range; the phenylmethyl that is formed via reaction 3b will likely react with toluene and H atoms, with both reactions recycling toluene.[30] Hence, these two reactions would not discernibly affect our modeled OH traces. As one of the decomposition products of TBHP is acetone, the reaction between phenylmethyl and acetone is also expected to occur. But estimates of the rate coefficient for this reaction[30] indicate that it is much too slow to be of any importance in our experiments. Another possible interfering reaction is that between phenylmethyl and OH. Using C_6H_5 + OH as a model,[7] we find that this reaction also is unlikely to have any perceptible effect on our measurements.

TABLE 4: Reactions Describing $C_6H_4CH_3$ Chemistry[a]

reaction	rate coeff [cm^3 mol^{-1} s^1]		
	A	*n*	*E*, cal/mol
$C_6H_5CH_3 + C_6H_4CH_3 \rightarrow C_6H_5CH_2 + C_6H_5CH_3$	7.9×10^{13}	0.0	12 000
$C_6H_5CH_3 + H \rightarrow C_6H_4CH_3 + H_2$	6.0×10^{8}	1.0	16 800
$C_6H_5CH_3 + O \rightarrow C_6H_4CH_3 + OH$	2.0×10^{13}	0.0	14 700
$C_6H_5CH_3 + HO_2 \rightarrow C_6H_4CH_3 + H_2O_2$	4.0×10^{11}	0.0	28 900
$C_6H_5CH_3 + CH_3 \rightarrow C_6H_4CH_3 + CH_4$	2.0×10^{12}	0.0	15 000
$C_6H_4CH_3 + O_2 \rightarrow O\ C_6H_4CH_3 + O$	2.6×10^{13}	0.0	6 100
$C_6H_4CH_3 + O_2 \rightarrow OC_6H_4O + CH_3$	3.0×10^{13}	0.0	9 000
$C_6H_4CH_3 + H \rightarrow C_6H_5CH_3$	1.0×10^{14}	0.0	0
$C_6H_4CH_3 + O \rightarrow OC_6H_4CH_3$	1.0×10^{14}	0.0	0
$C_6H_4CH_3 + OH \rightarrow HO\ C_6H_4CH_3$	1.0×10^{13}	0.0	0
$C_6H_4CH_3 + CH_3 \rightarrow$ xylene	1.2×10^{6}	1.96	−3 700
$C_6H_4CH_3 + HO_2 \rightarrow OC_6H_4CH_3 + OH$	5.0×10^{12}	0.0	0
$C_6H_4CH_3 + H \rightarrow C_6H_5CH_2 + H$	1.0×10^{13}	0.0	0

[a] All rate parameters from Bounaceur et al.[9]

We hence conclude that phenylmethyl chemistry does not affect our determination of a rate coefficient for reaction 3—C_6H_4-CH_3 reactions were therefore disregarded in this study. To confirm this conclusion, we added to the Pitz et al. mechanism $C_6H_4CH_3$ reactions from the recent toluene oxidation modeling study by Bounaceur et al.[9] (see Table 4) and remodeled our experimental OH profiles. As expected, there was no discernible effect on the simulated OH time histories, which indicates that phenylmethyl chemistry does not interfere with our measurements of k_3.

Acetone + OH Kinetics. The reaction between acetone and OH, reaction 6, was one of the secondary reactions encountered in the toluene + OH study. There has been just one kinetic study of this reaction at elevated temperatures.[20] The scarcity of high-temperature data, combined with the fact that the reaction shows pronounced non-Arrhenius behavior, resulted in a relatively high uncertainty estimate of a factor of 3 in its rate coefficient.[30] This, in turn, contributed to an uncertainty of about 25% in the rate coefficient of reaction 3, leading initially to an overall uncertainty of ±40% for k_3 at ∼1100 K. As the kinetics of OH radical attack on acetone are of general importance in combustion systems, we thus carried out extensive kinetic measurements of reaction 6 at elevated temperatures.

The reaction was studied at temperatures ranging from 982 to 1300 K, and total pressures between 1.52 and 1.80 atm. Reaction rate coefficients were once again extracted by matching modeled and measured OH time histories in the reflected shock region. The GRI Mech 3.0 mechanism[31] was used to model the reaction system. Acetone chemistry was incorporated into the mechanism from the detailed LLNL hydrocarbon oxidation model (a total of 23 reactions involving CH_3COCH_3, CH_3-$COCH_2$, and CH_3CO were added).[7,24] The only product channel considered in the modeling is the one leading to CH_3COCH_2 and H_2O because it has been shown[33] that these are the dominant products formed at temperatures greater than about 450 K. Nominal mixtures with 200 ppm of TBHP (and water) and 480−505 ppm of acetone in argon were prepared.

A typical OH concentration time history recorded for a mixture of 200 ppm of TBHP (and water) and 486 ppm of acetone in argon is shown in Figure 4a. Figure 4b, an OH radical sensitivity analysis, shows that there is strong isolation of the target reaction. There is, as expected, slight interference from the CH_3 + OH reaction system. For the experiment shown (1048 K and 1.77 atm), a rate coefficient of 3.35×10^{12} cm^3 mol^{-1} s^{-1} results in good agreement between model and experiment. Figure 4c presents an OH concentration profile for a higher temperature measurement at 1260 K (and 1.57 atm)—at these conditions, reaction 6 continues to be the dominant reaction, though interference from the CH_3 + OH system is greater than that for our lower temperature experiments. A detailed error analysis was carried out to set uncertainty limits on these measurements. Overall uncertainty bars of ±25% are estimated.

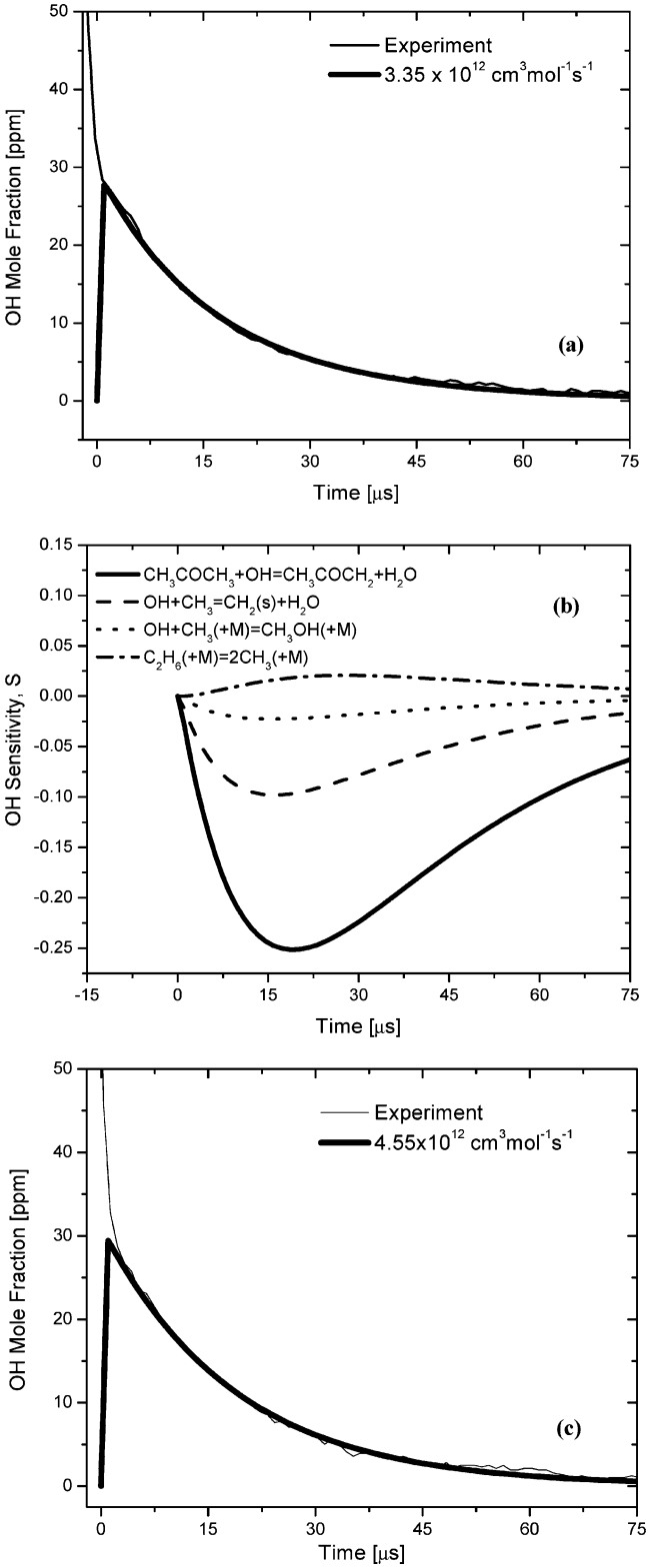

Figure 4. (a, b) Initial reflected shock conditions: 1048 K, 1.8 atm; 29.3 ppm TBHP, 486 ppm CH_3COCH_3, Ar: (a) OH concentration time history and (b) OH radical sensitivity analysis, $S = (dX_{OH}/dk_i)(k_i/X_{OH})$. (c) Initial reflected shock conditions: 1260 K, 1.57 atm; 31 ppm TBHP, 486 ppm CH_3COCH_3, Ar: OH concentration time history.

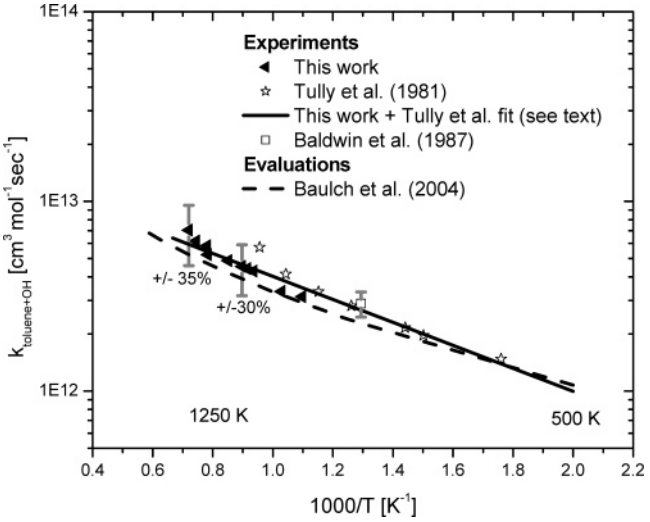

Figure 5. Arrhenius plot for $C_6H_5CH_3 + OH \rightarrow$ products at temperatures greater than 500 K.

Table 2 summarizes our measurements of $CH_3COCH_3 + OH \rightarrow CH_3COCH_2 + H_2O$.

The toluene + OH measurements were remodeled with the new acetone + OH data. There was no discernible effect on the rate coefficient of reaction 3, and this is because the rate coefficient for reaction 6 in the Pitz et al. model is in reasonable agreement (at high temperatures) with the current measurements (see Figure 6b). The new experimental data did allow us to lower the uncertainty estimate on reaction 6 from a factor of 3, to ±30%. This, consequently, resulted in lower uncertainty bars of ±30% on the rate coefficient of the reaction between toluene and OH (see Figure 3).

Comparison with Earlier Work. Figure 5 presents the current data along with earlier evaluations and measurements of reaction 3 at temperatures greater than about 500 K. Only a limited number of studies of this key reaction have been reported at elevated temperatures.[15,32] In Tully et al.,[15] OH radicals were generated by flash photolysis of H_2O at 165−185 nm, and the resulting fluorescence was monitored. Temperature and pressure ranged between 500 and 1050 K and 27−133 mbar, respectively. Studies of dueterated toluenes were also carried out to elucidate the variations of the reaction mechanism with temperature. In the Baldwin et al. study,[32] small amounts of toluene were added to $H_2 + O_2$ mixtures—measurements of the consumption of toluene and H_2 by gas chromatography facilitated the evaluation of rate coefficients for the reactions of toluene with OH, H, and O.

As is evident from Figure 5, the current high-temperature measurements of k_3 ($k_{3a} + k_{3b} + k_{3c}$) are consistent and in good agreement with the overall rate coefficient measurements of Tully et al. and Baldwin et al. The present data were fit with the lower temperature measurements of Tully et al. to the following two-parameter form, applicable over 570−1389 K:

$$k_3 = (1.62 \times 10^{13}) \exp(-1394/T\,[\mathrm{K}])\ [\mathrm{cm^3\,mol^{-1}\,s^{-1}}]$$

From Figure 5, we note that there appears to be slight non-Arrhenius behavior at temperatures greater than ~1000 K. But since this curvature is within experimental uncertainty and scatter, we decided not to use a three-parameter form for k_3—a two-parameter expression fits very well the current measurements with the Tully et al. data.

The reaction between acetone and OH radicals, like reaction 3, has not been extensively studied at elevated temperatures. In

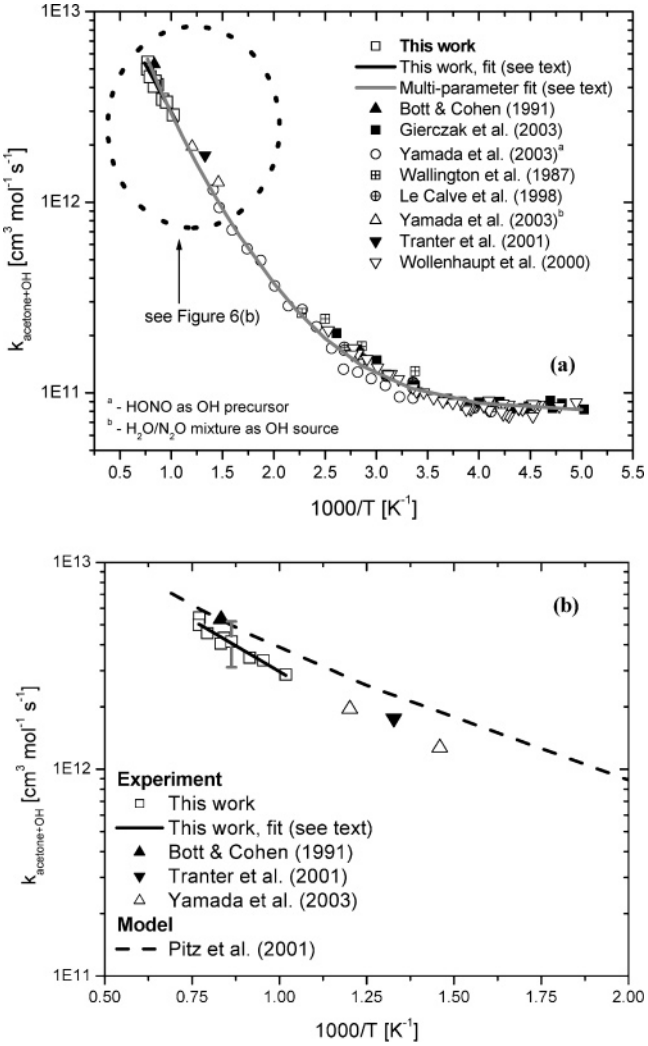

Figure 6. Arrhenius plot for $CH_3COCH_3 + OH \rightarrow$ products; (a) at all temperatures (200−2000 K) and (b) at moderate to high (500−2000 K) temperatures.

the only other direct, high-temperature measurement reported for this reaction,[20] resonance absorption detection of OH was used to measure the rate coefficient of reaction 6 under pseudo first-order conditions at 1200 K. Resonance radiation at 309 nm was produced by a microwave-powered discharge through a mixture of helium and water vapor flowing at 70 Torr through a quartz lamp. There have been several studies of this reaction at low to moderate temperatures though.[33−38] Figure 6 summarizes our and earlier measurements of reaction 6. Within experimental uncertainty, the current measurements agree very well with the Bott and Cohen data.[20] It is pertinent to note that, while at lower temperatures curvature in the Arrhenius plot is marked, at moderate to high temperatures, the experimental data points more or less lie along a line. A two-parameter fit of the current data, valid over the 982−1300 K temperature range, yields the following rate expression:

$$k_6 = (2.95 \times 10^{13}) \exp(-2297/T\,[\mathrm{K}])\ [\mathrm{cm^3\,mol^{-1}\,s^{-1}}]$$

A least-squares multi-parameter fit for the overall reaction rate coefficient of $CH_3COCH_3 + OH \rightarrow$ products, valid over the temperature range of 200−1300 K, is given below:

$$k_{ov} = 8.0 \times 10^{10} + (6.08 \times 10^{8})\, T^{1.41} \times \exp(-1289/T\,[\mathrm{K}])\ [\mathrm{cm^3\,mol^{-1}\,s^{-1}}]$$

Not included in this multi-parameter fit are the measurements of Yamada et al.,[33] because the authors state in their paper that there could exist a small systematic error in their rate measurements, possibly due to loss of acetone during transport through the reactor used in their experiments.

Conclusions

The reaction between toluene and OH was studied in reflected shock wave experiments by monitoring OH, using narrow line width ring dye laser absorption at 306.7 nm. Our high-temperature measurements are consistent with the lower temperature measurements of Tully et al.[15] The current measurements were fit with the Tully et al. data to the following two-parameter form, applicable between 570 and 1389 K:

$$k_3 = (1.62 \times 10^{13}) \exp(-1394/T\,[\mathrm{K}])\ [\mathrm{cm^3\,mol^{-1}\,s^{-1}}]$$

Detailed uncertainty analyses, taking into account mechanism-induced and experimental uncertainties, yielded an uncertainty estimate of ±30% at 1115 K.

The kinetics of OH radical attack on acetone was also studied at elevated temperatures. There is good agreement between the present work and the only other elevated temperature measurement reported in the literature by Bott and Cohen.[20] The current measurements were fit to the following Arrhenius form, applicable between 982 and 1300 K:

$$k_6 = (2.95 \times 10^{13}) \exp(-2297/\mathrm{T}\,[\mathrm{K}])\ [\mathrm{cm^3\,mol^{-1}\,s^{-1}}]$$

Detailed error analyses yielded an uncertainty estimate of ±25% at 1159 K.

Acknowledgment. This work was supported by the U.S. Department of Energy, Office of Basic Energy Sciences, with Dr. Frank Tully as contract monitor. The authors thank Dr. William Pitz of Lawrence Livermore National Laboratory and Prof. David Golden of Stanford University for advice and suggestions.

References and Notes

(1) Brezinsky, K. *Prog. Energy Combust. Sci.* **1986**, 12, 1.
(2) Goodger, E.; Vere, R. *Aviations Fuel Technology*; MacMillan Publishers Ltd.: London, UK, 1985.
(3) ASTM Special Technical Publication No. 225; American Society of Testing Materials: Philadelphia, PA, 1958.
(4) Emdee, J. J.; Brezinsky, K.; Glassman, I. *J. Phys. Chem.* **1992**, 96, 2151.
(5) Davis, S. G.; Wang, H.; Brezinsky, K.; Law, C. K. *Proc. Combust. Inst.* **1996**, 26, 1025.
(6) Lindstedt, R. P.; Maurice, L. Q. *Combust. Sci. Technol.* **1996**, 120, 119.
(7) Pitz, W. J.; Seiser, R.; Bozzelli, J. W.; Da Costa, I.; Fournet, R.; Billaud, F.; Battin-Leclerc, F.; Seshadri, K.; Westbrook, C. K. Second Joint Meeting, U.S. Sections of the Combustion Institute, Paper 253, 2001.
(8) Dagaut, P.; Pengloan, G.; Ristori, A. *Phys. Chem. Chem. Phys.* **2002**, 4, 1846.
(9) Bounaceur, R.; Da Costa, I.; Fournet, R.; Billaud, F.; Battin-Leclerc, F. *Int. J. Chem. Kinet.* **2005**, 37, 25.
(10) Vasudevan, V.; Davidson, D. F.; Hanson, R. K. *Proc. Combust. Inst.* **2004**, 30, 1155.
(11) Herbon, J. T.; Hanson, R. K.; Golden, D. M.; Bowman, C. T. *Proc. Combust. Inst.* **2002**, 29, 1201.
(12) Yu, C. L.; Frenklach, M.; Masten, D. A.; Hanson, R. K.; Bowman, C. T. *J. Phys. Chem.* **1994**, 98, 4470.
(13) Baulch, D. L.; Bowman, C. T.; Cobos, C. J.; Cox, R. A.; Just, Th.; Kerr, J. A.; Pilling, M. J.; Stocker, D.; Troe, J.; Tsang, W.; Walker, R. W.; Warnatz, J. *J. Phys. Chem. Ref. Data.* In press.
(14) Perry, R. A.; Atkinson, R.; Pitts, J. N., Jr. *J. Phys. Chem.* **1977**, *81*, 296.
(15) Tully, F. P.; Ravishankara, A. R.; Thompson, R. L.; Nicovich, J. M.; Shah, R. C.; Kreutter, N. M.; Wine, P. H. *J. Phys. Chem.* **1981**, *85*, 2262.
(16) Markert, F.; Pagsberg, P. *Chem. Phys. Lett.* **1993**, 209, 445.
(17) Knispel, R.; Koch, R.; Siese, M.; Zetzsch, C. *Ber. Bunsen-Ges. Phys. Chem*. **1990**, 94, 1375.
(18) Eng, R. A.; Gebert, A.; Goos, E.; Hippler, H.; Kachiani, C. *Phys. Chem. Chem. Phys.* **2002**, 4, 3989.
(19) Luther, K.; Troe, J.; Weitzel, K.-M. *J. Phys. Chem.* **1990**, 94, 6316.
(20) Bott, J. F.; Cohen, N. *Int. J. Chem. Kinet*. **1991**, 23, 1017.
(21) Vasudevan, V.; Davidson, D. F.; Hanson, R. K. *Int. J. Chem. Kinet*. **2005**, 37, 98.
(22) Kee, R. J.; Rupley, F. M.; Miller, J. A. *The Chemkin Thermodynamic Database*; Report No. SAND87-8215B.; Sandia National Laboratories: Livermore, CA, 1987.
(23) Jaynes, D. N.; Beam, B. H. *Appl. Opt.* **1969**, 8, 1741.
(24) Curran, H. J.; Gaffuri, P.; Pitz, W. J.; Westbrook, C. K. *Combust. Flame* **1998**, *114*, 149.
(25) Zhong, X.; Bozzelli, J. W. *Int. J. Chem. Kinet.* **1997**, 29, 893.
(26) Zhong, X. Ph.D. Thesis, New Jersey Institute of Technology, Newark, NJ, 1998.
(27) Zhong, X.; Bozzelli, J. W. *J. Phys. Chem.* **1998**, *102*, 3537.
(28) Benson, S. W.; O'Neal, H. E. *Kinetic Data on Gas-Phase Unimolecular Reactions*; National Bureau of Standards: Washington, DC, 1970; NSRDS-NBS 21.
(29) Choo, K. Y.; Benson, S. W. *Int. J Chem Kinet.* **1981**, 13, 833.
(30) Pitz, W. J. Personal communication, 2004.
(31) Smith, G. P.; Golden, D. M.; Frenklach, M.; Moriarty, N. W.; Eiteneer, B.; Goldenberg, M.; Bowman, C. T.; Hanson, R. K.; Song, S.; Gardiner, W. C., Jr.; Lissianski, V. V.; Qin, Z.: http://www.me.berkeley.edu/gri_mech/.
(32) Baldwin, R. R.; Scott, M.; Walker, R. W. *Proc. Combust. Inst.* **1986**, 21, 991.
(33) Yamada, T.; Taylor, P. H.; Goumri, A.; Marshall, P. *J. Chem. Phys.* **2003**, 119, 10600.
(34) Gierczak, T.; Gilles, M. K.; Bauerle, S.; Ravishankara, A. R. *J. Phys. Chem. A* **2003**, 107, 5014.
(35) Wollenhaupt, M.; Carl, S. A.; Horowitz, A.; Crowley, J. N. *J. Phys. Chem. A* **2000**, 104, 2695.
(36) Tranter, R. S.; Walker, R. W. *Phys. Chem. Chem. Phys.* **2001**, 3, 1262.
(37) Wallington, T. J.; Kurylo, M. J. *J. Phys. Chem. A* **1987**, 91, 5050.
(38) Le Calve, S.; Hitier, D.; Le Bras, G.; Mellouki, A. *J. Phys. Chem. A* **1998**, 102, 4579.